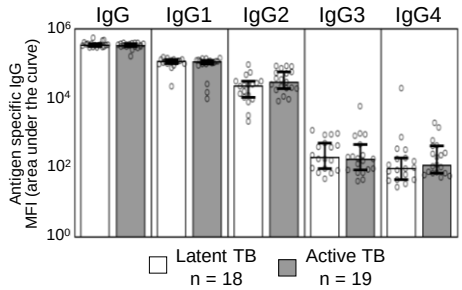

Supplemental Figure 1. No difference in RSV-specific IgG and subclasses between latent and active TB. Bar graphs show the median of the relative abundance of IgG for control RSV with 95% CI for individuals with latent and active TB. Statistical significance was determined by linear regression to adjust for sex and age. No *P*-values were ≤ 0.05.

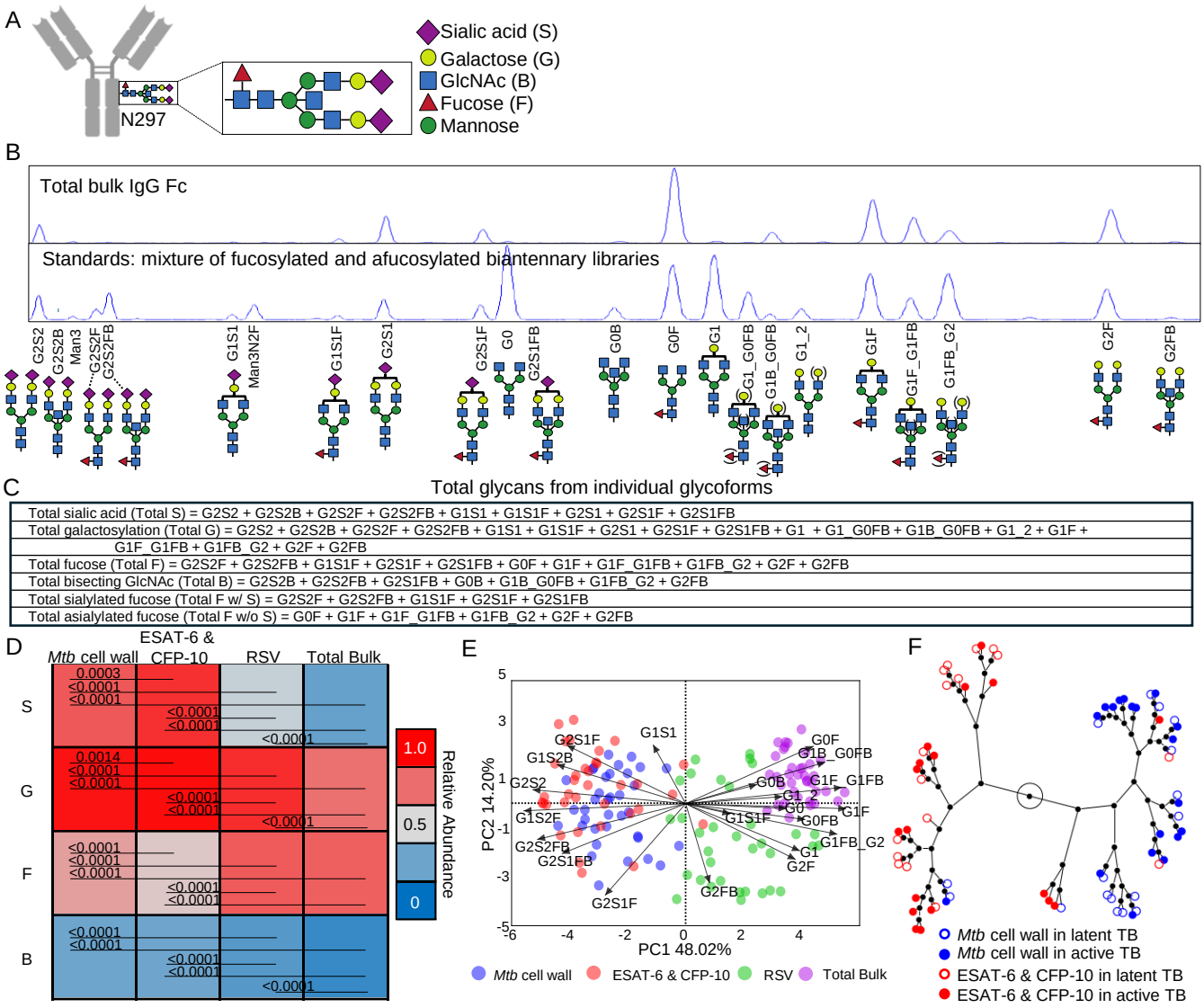

Supplemental Figure 2. Antigen specificity impacts IgG Fc domain N-glycosylation. (A) On a conserved N297 of the IgG Fc domain is a complex biantennary glycan structure composed of core mannose and N-acetylglucosamine on which variable amounts of galactose, sialic acid, and fucose are added. **(B)** Individual glycoforms on polyclonal IgG can be quantified by capillary electrophoresis using standards from biantennary glycan libraries. **(C)** Total glycans summarize individual glycoforms. **(D)** Heatmap shows the relative abundance of the glycans by antigen specificity with significance determined by Wilcoxon matched-pairs signed rank tests and *P*-values adjusted for multiple comparisons by controlling for the false discovery rate (Q=1%) using the two-stage step-up method of Benjamini, Krieger, Yekutieli. **(E)** Principal components analysis of individual IgG glycoforms from TB patients show separation by antigen specificities. Each dot summarizes the linear combination of antigen specific glycoforms of an individual patient. The loadings (arrows) show the coefficients of the linear combination of the individual glycoforms from which the principal components are constructed, demonstrating which individual glycoforms give the largest contribution to the components. **(F)** Constellation plot shows the relationships from hierarchical clustering of the glycan patterns for ESAT6 & CFP10 and *Mtb* cell wall IgG in latent and active TB.

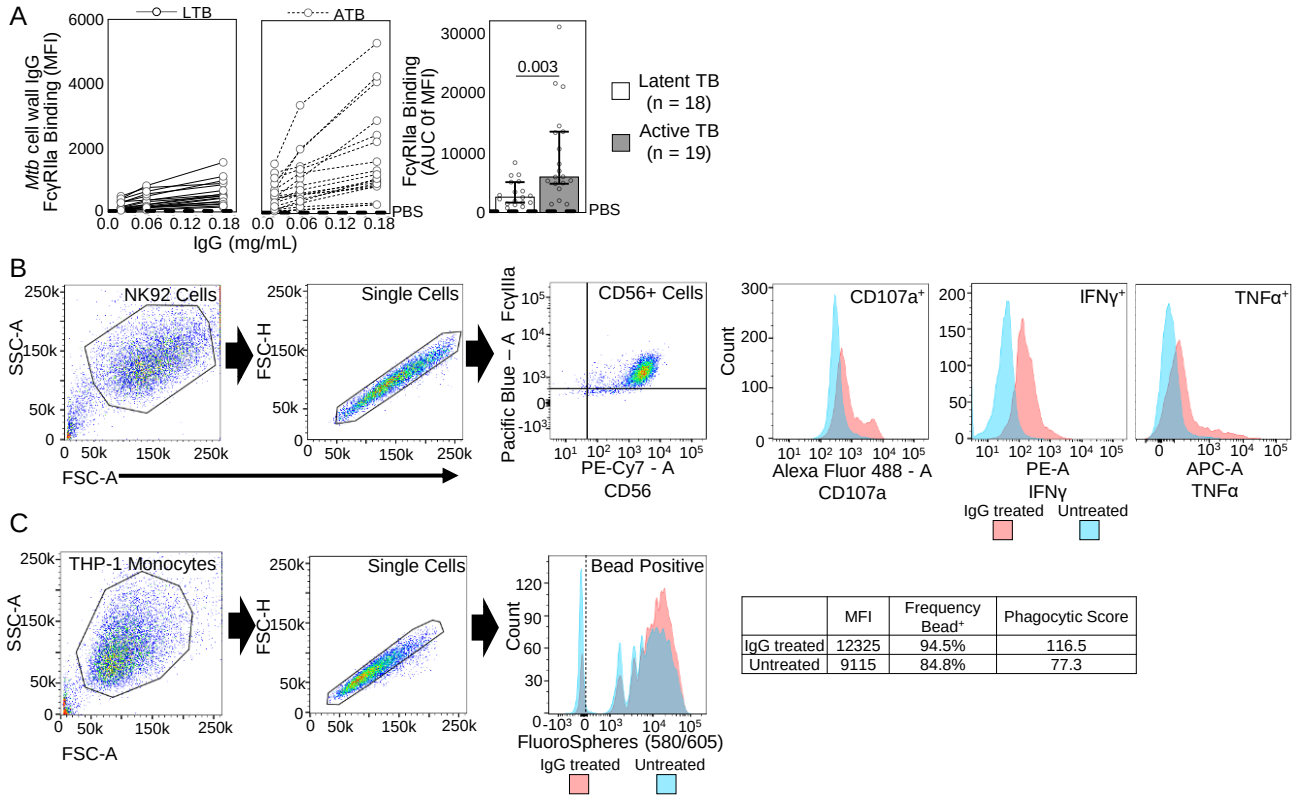

	MFI	Frequency Bead⁺	Phagocytic Score
IgG treated	12325	94.5%	116.5
Untreated	9115	84.8%	77.3

Supplemental Figure 3. High throughput approaches quantify antigen specific FcR binding and Fc effector functions in IgG isolated from individuals with TB. (A) Customized Luminex assays were used to measure the relative antigen specific IgG-FcγR binding in each patient sample across three dilutions to enhance sensitivity. A representative plot of the data is shown. Each line represents a single patient sample. The AUC of the MFI from IgG dilutions is used to summarize relative binding for each patient sample. The bold dashed line represents PBS control. Bar graphs show the median of with 95% CI for latent and active TB. Statistical significance was determined by linear regression to adjust for sex and age. **(B)** High throughput flow cytometry is used to measure antigen specific antibody dependent NK cell activation (ADNKA) in each individual patient sample. %NK CD56⁺ cells expressing CD107a, IFNγ, or TNFα mark activation in response to antigen specific IgG. **(C)** The human monocyte cell line THP-1 is used to quantitate antibody dependent cellular phagocytosis (ADCP) by determining the frequency and extent of antibody mediated uptake of antigen coated coated fluorescent beads.

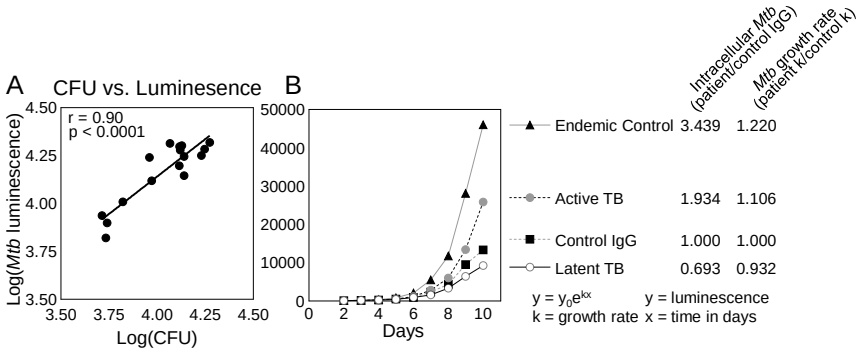

Supplemental Figure 4. Infection of macrophages by reporter strain of H37Rv captures differences in bacterial growth with treatment by latent and active TB IgG. (A) Log(*Mtb* luminescence) and Log(CFU) correlate as shown by Pearson. **(B)** Daily luminescence measurements of *Mtb* infected macrophages enable the determination of bacterial burden and growth rate by the exponential growth model.

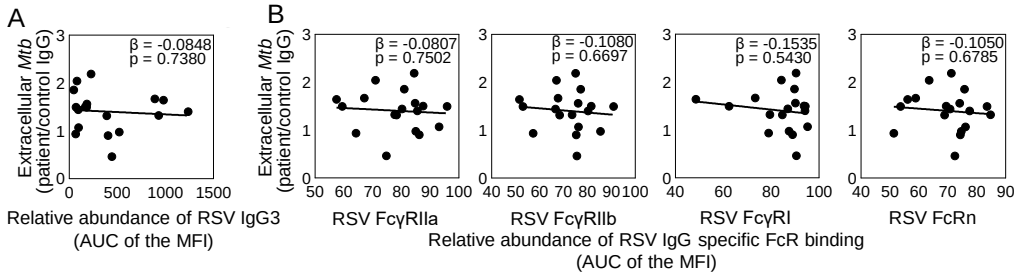

Supplemental Figure 5. RSV IgG3 and Fc receptor binding do not relate to extracellular *Mtb*. The absence of relationships between RSV IgG3 from latent TB and **(A)** *Mtb* burden and **(B)** Fc receptor binding as determined by simple linear regression is shown with no significant *P*-values.

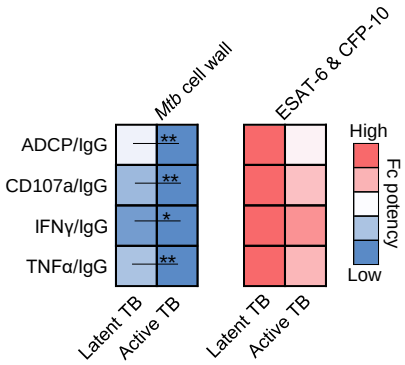

Supplemental Figure 6. *Mtb* cell wall, not ESAT-6 & CFP-10, IgG Fc potency is reduced in active compared to latent TB. Heatmap depicts ADCP and markers of ADNKA normalized by antigen specific IgG titers to determine functional potency. Statistical significance was determined by linear regression to adjust for sex and age. *$P \leq 0.05$ and **$P \leq 0.01$.

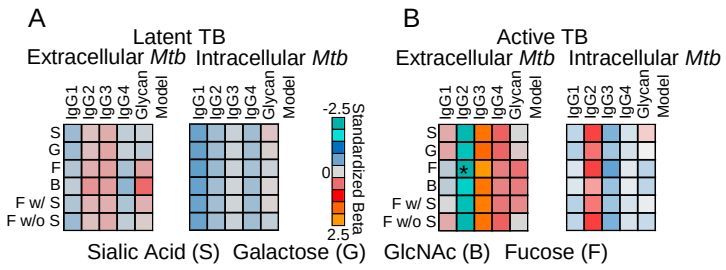

Supplemental Figure 7. ESAT-6 & CFP-10 subclasses and glycans have minimal relationships with *Mtb* burden. Heatmaps show that in **(A)** latent TB and **(B)** active TB, ESAT6 & CFP10 subclasses combined with glycans have limited relationships to intracellular and extracellular *Mtb* burden as determined by multiple linear regression. **P* ≤0.05.

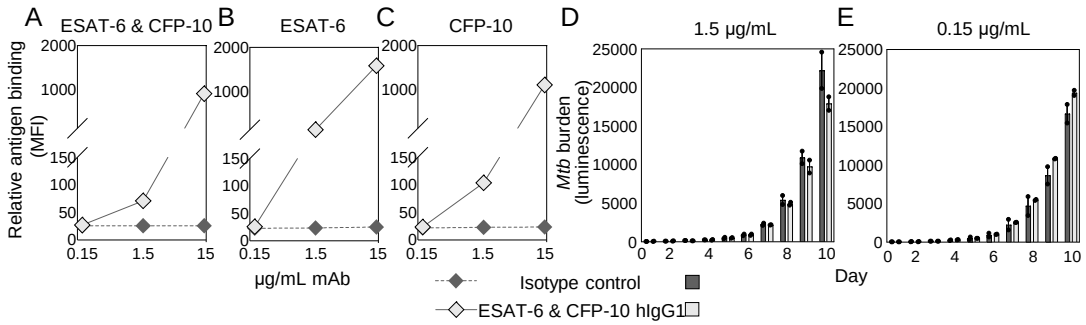

Supplemental Figure 8. A human IgG1 mAb binds ESAT-6 & CFP-10 and does not inhibit intracellular *Mtb* at low doses. Luminex demonstrates relative binding of mAb to ESAT-6 and isotype control CR3022 anti-SARS-CoV-2 RBD hIgG1 to (A) ESAT-6 & CFP-10, (B) ESAT-6, and (C) CFP-10. Treatment of *Mtb* infected macrophages at the low doses of **(D)** 1.5 or **(E)** 0.15µg/mL mAb had limited impact on intracellular burden during macrophage infection. Mean and SEM are shown. There were no significance differences as determined by unpaired t-test.